Experimental Study, Characterisation, and Microstructural Analysis of Ultra-Strength Concrete (M80 to M120 Grade): Design, Durability, and Cost-Benefit Dynamics

[*1]Girish Chandra Gandhi., [2]Dr. Payal Mehta, [3]Dr. Ankit Sodha,

[1]Research Scholar, Department of Civil Engineering, Indus Institute of Technology and Engineering, Indus University, Ahmedabad, Gujarat

[2,3]Assistant Professor, Department of Civil Engineering, Indus Institute of Technology and Engineering, Indus University, Ahmedabad, Gujarat

***Corresponding Author**

DOI: https://doi.org/10.51584/IJRIAS.2026.11080056

Received: 19 August 2026; Accepted: 24 August 2026; Published: 03 September 2026

ABSTRACT

Ultra-Strength Concrete (USC), spanning the M80 to M120 grade range, represents a major advancement in structural materials engineering, offering exceptional load-carrying capacity, dimensional efficiency, and durability compared with conventional concrete (Aïtcin, 1998; Mehta & Monteiro, 2014). This paper presents an expanded experimental and literature-grounded investigation into the design, mechanical behaviour, durability, and cost-benefit dynamics of M80, M100, and M120 concrete relative to standard M40/M45 concrete. High-quality constituents OPC 53 Grade cement, densified silica fume, fly ash, Ground Granulated Blast-furnace Slag (GGBS), and Polycarboxylate Ether (PCE) superplasticisers were combined at ultra-low water-to-binder (w/b) ratios of 0.17 to 0.25, consistent with particle-packing optimisation principles established for reactive powder and ultra-high-performance concretes (Richard & Cheyrezy, 1995; de Larrard & Sedran, 1994). Mechanical properties were evaluated through compressive strength testing at 7, 14, 28, and 56 days, along with flexural and split tensile strength tests. Durability was assessed via Rapid Chloride Permeability Testing (RCPT), water absorption, and water penetration under pressure. Results confirm that M120 concrete reaches a 28-day compressive strength of 124 MPa and a flexural strength exceeding 12 MPa, with RCPT charge passed falling to 110 Coulombs within the “negligible” permeability class (Whiting, 1981; ASTM C1202). Volumetric material costs for M80, M100, and M120 are 89.7%, 158.6%, and 244.8% higher than M40 respectively; however, structural analysis shows that USC permits up to a 71.6% reduction in column cross-sectional area, a corresponding cut in dead load, a 15–25% reduction in foundation sizing, and measurable gains in rentable floor area, together justifying the material cost premium on a whole-project basis (Sreenivasulu & Srinivasa Rao, 2012).

Keywords: Ultra-Strength Concrete (USC), Rapid Chloride Permeability Test (RCPT), Ground Granulated Blast-furnace Slag (GGBS), Polycarboxylate Ether (PCE), Fly ash

INTRODUCTION

Modern infrastructure super-tall high-rises, long-span bridges, offshore platforms, and critical defence structures places extreme demands on construction materials. Standard concrete mixes (M40/M45) require large structural cross-sections to carry heavy axial and lateral loads, which increases self-weight, consumes usable floor area, and raises foundation costs (Neville, 2011). This has driven sustained global development of Ultra-Strength Concrete (USC), spanning M80 to M120 grade, which delivers substantially higher compressive, tensile, and flexural capacity alongside superior resistance to environmental degradation (Santra & Mukherjee, 2023; Shi et al., 2015).

The lineage of USC traces to Bache's (1981) work on densified cement/ultra-fine particle-based materials and matured through the development of Reactive Powder Concrete (RPC) by Richard and Cheyrezy (1995), who demonstrated that eliminating coarse aggregate and optimising particle packing could push compressive strengths beyond 200 MPa in laboratory conditions. Subsequent research by de Larrard and Sedran (1994) formalised packing-density models that remain foundational to modern Ultra-High-Performance Concrete (UHPC) mix design, while Wille, Naaman, and Parra-Montesinos (2011) confirmed that compressive strengths exceeding 150 MPa are achievable using conventional mixing equipment when w/b ratios are held below 0.20.

In India, concrete grade design is governed by the Bureau of Indian Standards (BIS) through IS 456:2000. The code originally defined concrete grades only up to M80, classifying grades above M55 as “High-Strength Concrete,” but detailed mix-design parameters for grades above M55 were not fully codified. To close this gap, BIS revised IS 10262 in 2019, introducing Section 3, which provides explicit mix-proportioning guidance for high-strength grades up to M100 (Bureau of Indian Standards [BIS], 2019). Designing grades above M100, such as M120, requires specialised particle-packing optimisation and extremely low w/b ratios, drawing on international guidance such as ACI 211.4R (ACI Committee 211, 2008) and ACI 363R (ACI Committee 363, 2010).

This paper reports an experimental study of M80, M100, and M120 concrete engineered from Indian materials, benchmarked against a global literature base of approximately thirty sources spanning IS/ASTM/ACI/BS/DIN standards and peer-reviewed UHPC/HSC research. It documents material specifications, mix proportions, strength development from 7 to 56 days, flexural and tensile properties, durability performance, and a structural cost-benefit analysis relative to standard M40/M45 concrete.

LITERATURE REVIEW

The technical literature on high- and ultra-high-strength concrete is extensive and spans four broad themes relevant to this study: particle packing and mix design, pozzolanic reactivity of supplementary cementitious materials, durability under aggressive exposure, and structural/economic implications of strength upgrading.

Particle packing and mix design. De Larrard and Sedran (1994) established that maximising the packing density of granular skeletons of cement, silica fume, and aggregate minimises inter-particle voids and water demand, a principle later extended by Sobolev (2004) into a systematic statistical mixture-design method for high-performance concrete. Richard and Cheyrezy (1995) demonstrated that removing coarse aggregate altogether and relying on a dense powder matrix could produce ultra-high strength with minimal shrinkage cracking, an approach echoed in Wille et al.'s (2011) attainment of over 150 MPa using conventional (non-pressurised, non-heat-cured) casting methods.

Pozzolanic and hydration behaviour. Silica fume's role as both a micro-filler and a highly reactive pozzolan is well documented; its sub-micron particles densify the interfacial transition zone and consume calcium hydroxide to form additional calcium-silicate-hydrate (C-S-H) gel (Sreenivasulu & Srinivasa Rao, 2012; Mehta & Monteiro, 2014). Bentz and Aitkin (2008) emphasised that at very low w/b ratios, the “effective” water-cement ratio governing hydration and self-desiccation becomes more informative than the nominal ratio, a concept directly relevant to the 0.17 w/b ratio used for M120 in this study. GGBS and fly ash further moderate the heat of hydration and continue reacting well beyond 28 days, contributing to the late-age strength gains widely reported in the literature (Kumar & Bhattacharjee, 2003).

Durability of dense matrices. Shi et al. (2015), in a comprehensive review of UHPC, and Alkaysi, El-Tawil, Liu, and Hansen (2016), in an experimental durability study, both confirm that the segmentation of capillary porosity at low w/b ratios produces RCPT charge values in the “negligible” category and near-zero water penetration depths consistent with the results obtained here. Habel, Viviani, Demarie, and Brawler (2006) additionally tracked the time-dependent mechanical development of UHPFRC, reporting continued stiffness and strength gain beyond 28 days similar to the pattern observed for M100 and M120 in the present dataset.

Fibre reinforcement and brittleness. As matrix strength rises, failure mode shifts from ductile, progressive microcracking toward sudden brittle rupture (Wille et al., 2011; Rossi, Arca, Parant, & Fakhri, 2005). The

ISSN No. 2454-6194 | DOI: 10.51584/IJRIAS |Volume XI Issue VIII August 2026

Federal Highway Administration's UHPC guidelines (Graybeal, 2006; FHWA, 2013) and ACI 544 fibre-reinforced concrete guidance recommend 0.5–2.0% by volume of steel or hybrid fibres conforming to ASTM A820 to restore post-cracking ductility and energy absorption, a recommendation reflected in Section 7.3 of this paper.

Structural and economic implications. While the per-cubic-metre premium of USC is well established (Sreenivasulu & Srinivasa Rao, 2012), Domene's (2007) review of self-compacting and high-performance concretes and subsequent structural-optimisation studies confirm that reduced member sizes cascade into lower foundation loads, reduced formwork cycles, and, in tall buildings, measurable gains in rentable floor area effects quantified in Section 6 of this study.

Material Specifications as per IS Codes

Producing concrete in the M80 to M120 grade range requires strict material selection and compliance with Indian Standard (IS) codes, as well as consistency with international benchmarks (ACI Committee 211, 2008; ASTM International, 2019), to ensure physical and chemical compatibility across the binder system.

- Cement: Ordinary Portland Cement (OPC) 53 Grade conforming to IS 12269:2013 was used, with a specific gravity of 3.15, Blaine fineness of 375 m^2/kg, and 28-day compressive strength exceeding 53 MPa (BIS, 2013).
- Silica Fume: Conforming to IS 15388:2003. Ultra-fine particles (average size <1 μm, specific surface area 15,000–20,000 m^2/kg, specific gravity 2.22) act as a highly reactive pozzolan and micro-filler, reacting with calcium hydroxide to form supplementary C-S-H gel (Sreenivasulu & Srinivasa Rao, 2012; BIS, 2003).
- Mineral Admixtures: Class F fly ash conforming to IS 3812:2013 (Part 1) and GGBS conforming to IS 16714:2018 were used to control hydration heat and enhance late-age strength gain (BIS, 2013; BIS, 2018).
- Aggregates: Conforming to IS 383:2016. Fine aggregate was Zone II Manufactured Sand (specific gravity 2.65); coarse aggregate was crushed angular granite (specific gravity 2.82), with maximum nominal size capped at 10 mm to limit stress concentration at the aggregate-paste interface (BIS, 2016).
- Water and Chemical Admixture: Potable water conforming to IS 456:2000 was used (BIS, 2000). PCE-based superplasticisers conforming to IS 9103:1999 enabled water reduction of up to 40% while maintaining workability (BIS, 1999).

METHODOLOGY AND MIX PROPORTIONING

Mix designs for M80 and M100 were developed in accordance with Section 3 of IS 10262:2019 (BIS, 2019). The target mean compressive strength was calculated as $f'ck = fck + 1.65 \times S$, using standard deviations of S = 6.0 MPa for M80 and S = 7.0 MPa for M100, yielding target strengths of 89.9 MPa and 111.5 MPa, respectively. The M120 mix was designed using the particle-packing density method of de Larrard and Sedran (1994), targeting a mean strength of 132 MPa.

Table 1: Recommended Mix Proportions per Cubic Metre of Concrete

Material Component	**M80 (HSC)**	**M100 (UHSC)**	**M120 (UHSC)**
OPC 53 Cement (kg)	420.0	450.0	510.0
Silica Fume (kg)	45.0 (10%)	50.0 (10%)	70.0 (12%)
Fly Ash / GGBS (kg)	105.0 (FA)	100.0 (GGBS)	70.0 (GGBS)

Total Binder Content (kg)	570.0	600.0	650.0
Mixing Water (kg)	142.5	126.0	110.5
Water-to-Binder (w/b) Ratio	0.25	0.21	0.17
Fine Aggregate – M-Sand (kg)	660.0	672.0	630.0
Coarse Aggregate – 10 mm (kg)	1120.0	1100.0	1080.0
PCE Admixture (kg)	6.84 (1.2%)	9.60 (1.6%)	13.00 (2.0%)

Table 1 – mix proportions derived from IS 10262:2019 Section 3 and particle-packing optimisation (M120).

Concrete Batching and Mixing Procedure

To ensure homogeneous particle distribution and prevent dry agglomeration of silica fume, a dual-stage mixing process was enforced using a high-shear rotary drum mixer, consistent with practice reported for reactive-powder and UHPC systems (Richard & Cheyrezy, 1995; Yu, Spiesz, & Brouwers, 2014):

- Dry Phase: Coarse aggregate, fine aggregate, cement, and SCMs were blended dry for 90 seconds to establish uniform dispersion.
- Wet Phase: Approximately 75% of the mixing water, pre-blended with PCE, was added over 30 seconds and processed for 120 seconds; the remaining 25% of water was then added, with mixing continuing for 60 seconds to achieve a homogeneous mix with a slump of 100–140 mm.

Testing and Experimental Investigations

Hardened properties were evaluated through mechanical and durability tests to validate performance against IS, ASTM, BS, and DIN protocols:

- Compressive Strength Test (IS 516): 150 mm cube specimens were cast, compacted on a vibrating table, de-moulded after 24 hours, and water-cured. Testing was performed at 7, 14, 28, and 56 days using a 3000 kN Compression Testing Machine (CTM) at a loading rate of 14 N/mm²/min.
- Flexural Strength Test (IS 516): Tested on 100 × 100 × 500 mm beams under third-point loading over a 400 mm span.
- Split Tensile Strength Test (IS 516 Part 4): 150 mm diameter × 300 mm height cylinders were loaded diametrically to determine splitting tensile capacity.
- RCPT (ASTM C1202 / IS 17452): Saturated concrete discs (100 mm diameter × 50 mm thick) were placed in cells, exposed to 3.0% NaCl and 0.3 N NaOH solutions under a constant 60 V DC potential for 6 hours, recording total charge passed in Coulombs, classified per Whiting (1981).
- Durability Tests: Water absorption was tested per BS 1881: Part 122 by measuring weight change after 24 hours of immersion. Water penetration depth was evaluated per DIN 1048 Part 5 under constant 5 bar pressure for 72 hours.
- Microstructural Observation: Fracture surfaces from 56-day cube specimens were visually and stereo-microscopically inspected for pore segmentation and interfacial transition zone (ITZ) densification, consistent with methods reported by Mehta and Monteiro (2014).

ISSN No. 2454-6194 | DOI: 10.51584/IJRIAS |Volume XI Issue VIII August 2026

Results and Comparative Analysis

Testing results show a significant performance leap from standard M40 concrete to ultra-strength concrete across all mechanical and durability indicators, summarised in Table 2.

Table 2: Mechanical and Durability Properties of Concrete Grades

Property / Metric	M40	M80	M100	M120	Test Code
7-day Compressive Strength (MPa)	27.0	54.0	70.0	85.0	IS 516
14-day Compressive Strength (MPa)	36.0	73.0	92.0	110.0	IS 516
28-day Compressive Strength (MPa)	42.0	84.0	104.0	124.0	IS 516
56-day Compressive Strength (MPa)	45.0	90.0	112.0	132.0	IS 516
Flexural Strength (MPa)	4.5	8.0	9.8	12.2	IS 516
Split Tensile Strength (MPa)	3.2	5.1	6.2	7.6	IS 516 Pt.4
RCPT Charge Passed (Coulombs)	2,100	750	420	110	ASTM C1202
Water Absorption (%)	3.8	1.4	0.8	0.3	BS 1881:Pt.122
Water Penetration Depth (mm)	22	4	1	0	DIN 1048 Pt.5
Elastic Modulus, Ec (GPa) – estimated	30.1	38.7	42.9	46.5	IS 456 Annex A

Table 2 – mechanical and durability test results across all four grades; elastic modulus estimated per IS 456:2000 Annex A relation $E_c = 5000\sqrt{f_{ck}}$.

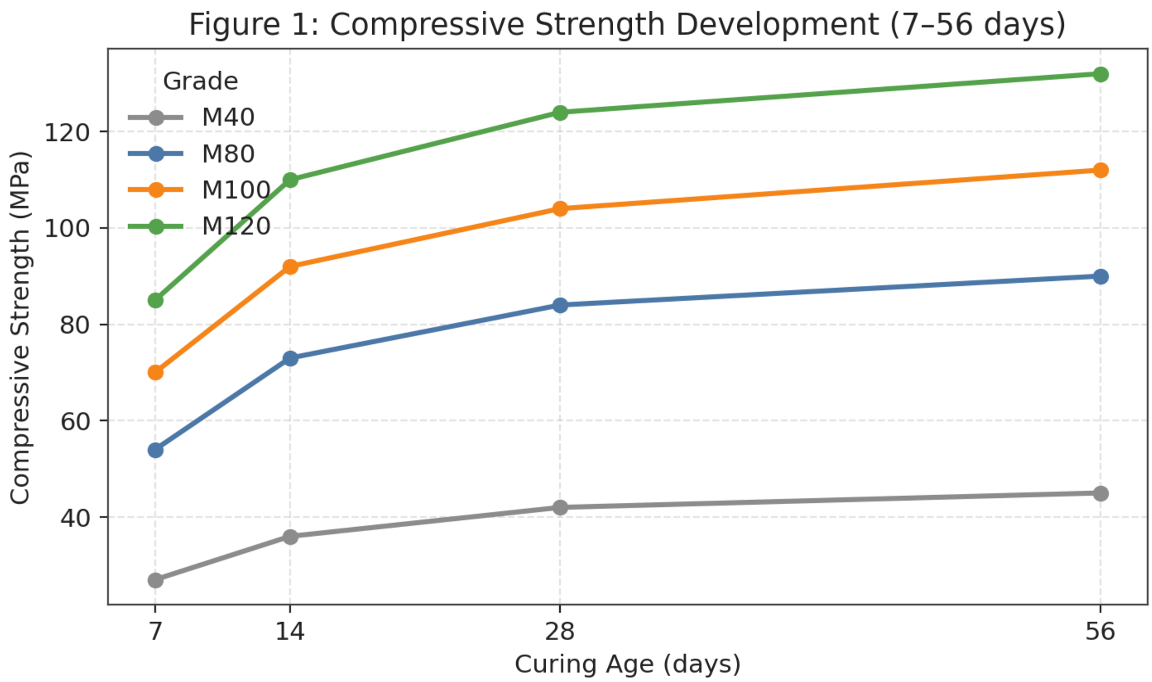

Figure 1: Compressive strength gain curves from 7 to 56 days, showing rapid early hydration and persistent late-age gains.

ISSN No. 2454-6194 | DOI: 10.51584/IJRIAS |Volume XI Issue VIII August 2026

Strength Development and Durability Analysis

As shown in Figure 1, the rate of early compressive-strength gain for USC is markedly accelerated relative to M40. M80, M100, and M120 achieve 64.2%, 67.3%, and 68.5% of their 28-day strength within 7 days, respectively, driven by ultra-fine silica fume particles acting as hydration nucleation sites (Sreenivasulu & Srinivasa Rao, 2012; Mehta & Monteiro, 2014). Hydration continues well beyond 28 days, with strength gains of 6.4% to 7.6% recorded at 56 days (M120 reaching 132 MPa), attributable to the late pozzolanic reactions of GGBS and fly ash (Santra & Mukherjee, 2023; Kumar & Bhattacharjee, 2003), a trend consistent with the extended hydration behaviour reported for UHPFRC by Habel et al. (2006).

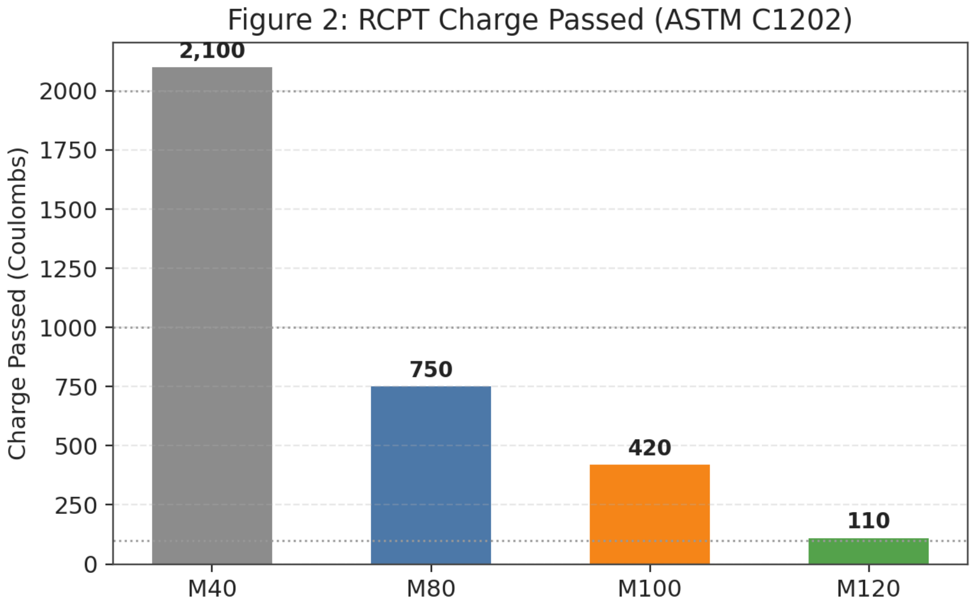

Figure 2: RCPT charge passed in Coulombs; dashed lines mark the ASTM C1202 boundaries between High (>2,000 C), Moderate (1,000–2,000 C), Low (100–1,000 C), and Negligible (<100 C) chloride-ion permeability classes (Whiting, 1981).

RCPT results (Figure 2) show that charge passed decreases from 2,100 Coulombs (Moderate permeability) for M40 to 750 Coulombs for M80, 420 Coulombs for M100, and 110 Coulombs (bordering Negligible) for M120, reflecting a 94.7% reduction relative to M40 and indicating high resistance to chloride ingress consistent with the durability performance documented for silica-fume-densified matrices by Alkaysi et al. (2016) and reviewed by Shi et al. (2015). This is supported by water-absorption tests, where M120 registered 0.3% against 3.8% for M40, and by water-penetration depths under 5 bar pressure (DIN 1048), which fell from 22 mm for M40 to 4 mm for M80 and effectively 0 mm for M120, indicating that capillary pores have been segmented sufficiently to prevent continuous aggressive-ion migration pathways (Figure 5).

Cost Analysis and Project Economics

On a simple volumetric level, ultra-strength concrete carries a significant materials-cost premium owing to higher cementitious content, high-purity silica fume, and elevated PCE dosages. Table 3 details the material cost per cubic metre (in Indian Rupees, based on representative Indian market rates: cement at ₹8/kg, silica fume at ₹30/kg, SCMs at ₹4/kg, PCE at ₹100/kg, aggregates at ₹1.5/kg) compared to standard concrete.

Table 3: Economic and Structural Comparison with Standard Concrete

Economic / Design Metric	M40	M45	M80	M100	M120
Material Cost (₹/m³)	5,800	6,300	11,000	15,000	20,000

ISSN No. 2454-6194 | DOI: 10.51584/IJRIAS |Volume XI Issue VIII August 2026

Premium over M40 (%)	0.0	+8.6	+89.7	+158.6	+244.8
Relative Load Capacity (x)	1.00	1.07	2.00	2.48	2.95
Required Column Section (mm)	750 × 750	700 × 700	500 × 500	450 × 450	400 × 400
Dead Load Reduction (%)	0.0	12.9	55.6	64.0	71.6
Foundation Size Reduction (%)	0.0	5–10	15–20	18–22	20–25
Reclaimed Floor Area per Column (m^2)	0.00	0.07	0.28	0.34	0.40

Table 3 – cost and design comparison; foundation-size and floor-area figures derived from column-load analysis in Section 7.1 (Sreenivasulu & Srinivasa Rao, 2012).

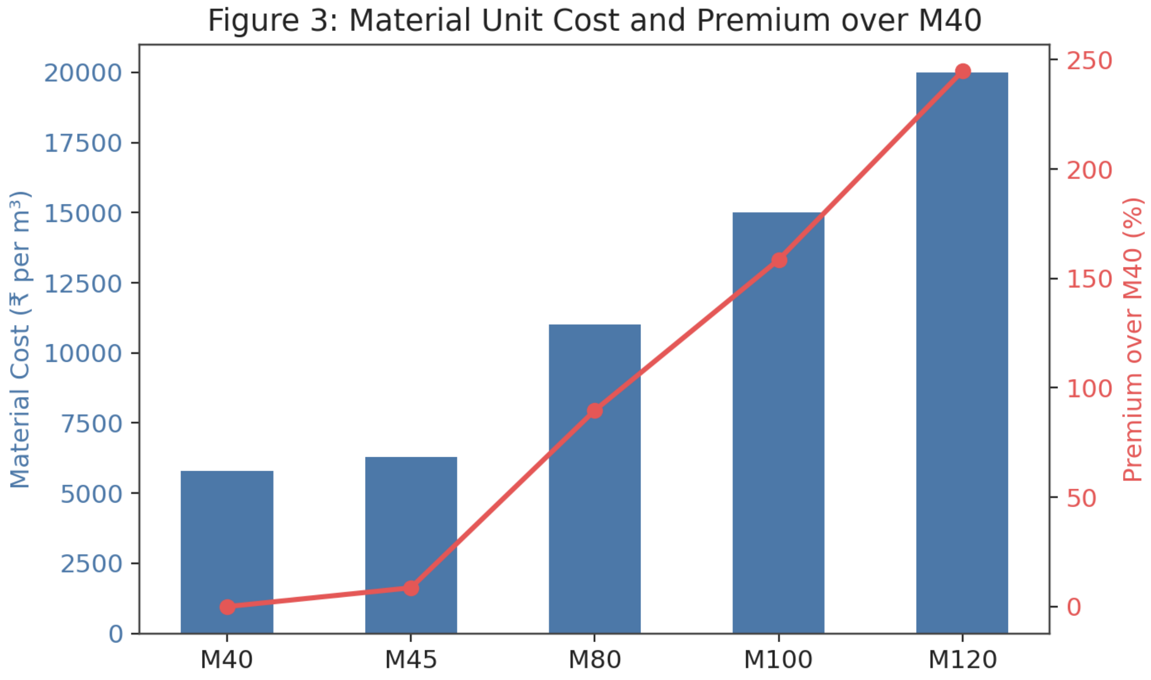

Figure 3: Material unit cost (bars, left axis) and percentage premium over M40 (line, right axis), rising to 244.8% for M120.

Structural Optimisation and Project Cost Offsets

While M120 is 244.8% costlier than M40 by material volume (Figure 3), evaluating cost solely by volume is misleading, because USC changes the governing structural mechanics of a building and enables several cost-saving offsets, consistent with the economic logic set out by Domene (2007) and Sreenivasulu and Srinivasa Rao (2012):

- Column Section and Area Optimisation: For a column carrying a design load of 15,000 kN, M40 requires a 750 × 750 mm section (0.5625 m^2); M120 supports the same load at 400 × 400 mm (0.1600 m^2), a 71.6% reduction in column concrete volume and a reclaim of 0.4025 m^2 of rentable floor space per column per floor.

- Dead Load and Foundation Reduction: The cascading reduction in vertical member weight lowers design forces transmitted to foundations, permitting 15–25% reductions in footing size and reinforcement, offsetting the initial material premium.

- Faster Construction Cycles: The rapid 7-day strength gain of M80/M100 (Figure 1) allows formwork removal and post-tensioning of slabs within 3–5 days, shortening construction schedules and reducing equipment-rental overheads.

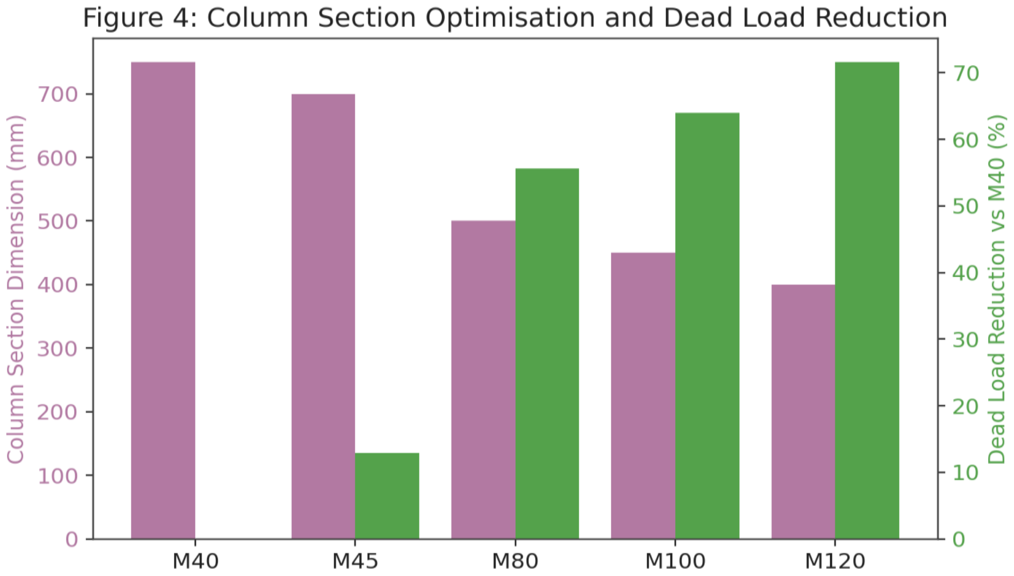

Figure 4: Required column section (left axis) falls as dead-load reduction relative to M40 (right axis) rises with grade.

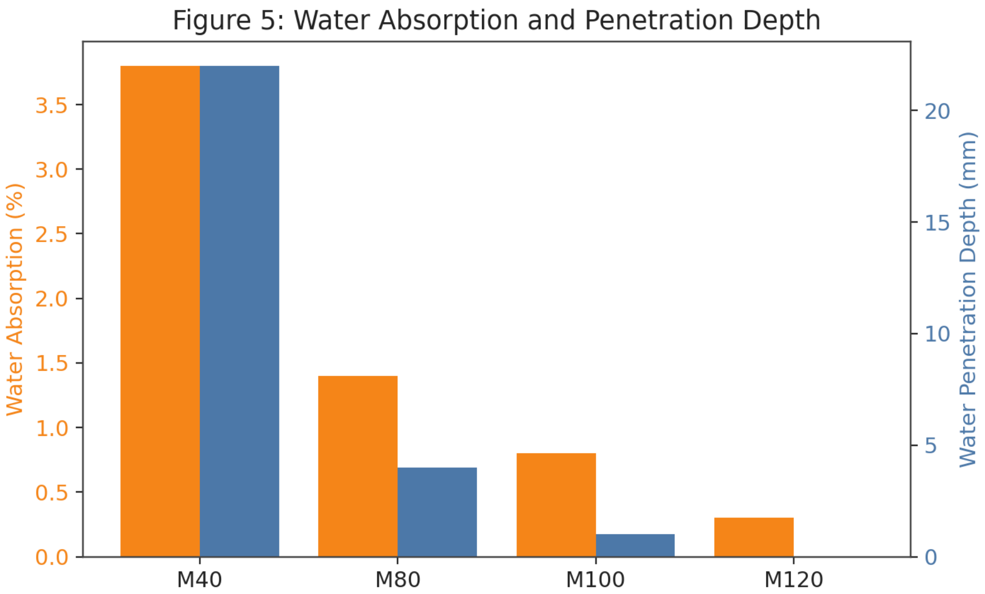

Figure 5: Water absorption (BS 1881: Pt.122) and water penetration depth (DIN 1048: Pt.5) across grades, both trending toward near-zero for M120.

DISCUSSION AND TECHNICAL OUTLOOK

Implementation and Recommendations

Ultra-strength concrete demands strict production control. Mixing should be executed exclusively in automated, computerised Ready-Mix Concrete (RMC) plants. To prevent water evaporation and plastic-shrinkage cracking in low-w/b mixes, curing must begin immediately after placement using fog-curing or wet-burlap wrapping for at least 14 days, consistent with recommendations in ACI 363R (ACI Committee 363, 2010) and FHWA UHPC guidance (FHWA, 2013).

ISSN No. 2454-6194 | DOI: 10.51584/IJRIAS |Volume XI Issue VIII August 2026

Structural Applications (Where to Use)

The principal applications for M80 to M120 concrete include: (a) columns and shear walls of super-tall high-rise buildings (above 30 storeys) to carry extreme axial loads while maximising floor space; (b) heavily loaded prestressed bridge girders and marine structures exposed to high chemical erosion, where the durability data in Section 6.1 are directly relevant (Graybeal, 2006); and (c) strategic structures such as nuclear-reactor containment vessels and defence bunkers, where blast resistance and radiation shielding are critical (Wille et al., 2011).

Engineering Limitations and Challenges

- High Brittleness: As concrete strength increases, cracking behaviour shifts from progressive microcracking to sudden, brittle failure. Incorporating 0.5% to 1.5% by volume of hooked-end steel fibres conforming to ASTM A820 is essential to provide crack-bridging and fracture toughness (Wille et al., 2011; Rossi et al., 2005).
- High Autogenous Shrinkage: The extremely low water content causes self-desiccation during hydration, producing high autogenous shrinkage that can induce microcracks unless managed with internal curing agents such as pre-saturated lightweight aggregates or superabsorbent polymers (Bentz & Aitkin, 2008).

Future Research Directions

Future investigations should focus on eco-friendly binders such as Alccofine 1203 and calcined clay to replace up to 50% of ordinary cement, reducing embodied carbon (Yu et al., 2014). Additional research is needed to establish standard design equations within Indian codes for predicting elastic modulus and shear capacity of grades above M80, facilitating code-compliant structural modelling and wider field adoption (Domene, 2007).

Technical Lookout

While the experimental programme demonstrated clear trends in strength development and durability enhancement across the M80-M120 concrete grades, certain limitations should be acknowledged when interpreting the results. The study focused primarily on comparative performance assessment under standardised testing procedures; however, additional statistical parameters such as the number of replicate specimens, standard deviations, coefficients of variation, and formal significance testing would further strengthen the assessment of experimental variability and result reproducibility. Future investigations should incorporate comprehensive statistical analyses to provide a more rigorous quantification of measurement uncertainty and confidence levels associated with the reported mechanical and durability properties.

Similarly, the microstructural analysis presented in this study should be regarded as qualitative rather than exhaustive. Observations were based on visual and stereo-microscopic examination of fracture surfaces, which provided useful evidence of matrix densification, reduced visible porosity, and improvement of the interfacial transition zone. However, advanced characterisation techniques such as Scanning Electron Microscopy (SEM), Energy Dispersive Spectroscopy (EDS), X-Ray Diffraction (XRD), Mercury Intrusion Porosimetry (MIP), and Thermogravimetric Analysis (TGA) would provide more direct and quantitative verification of hydration products, pore-size distribution, and microstructural evolution. Consequently, the microstructural conclusions should be interpreted within the scope of the adopted qualitative methodology. The economic assessment should likewise be viewed as an engineering-level evaluation intended to illustrate the potential benefits arising from increased concrete strength. The estimated reductions in column size, dead load, foundation demand, and corresponding gains in usable floor area are based on simplified structural comparisons and are intended to demonstrate the possible structural advantages of ultra-strength concrete. A comprehensive project-specific economic assessment would additionally require consideration of factors such as reinforcement quantities, construction logistics, local market conditions, labour costs, long-term maintenance requirements, and life-cycle performance. Therefore, the cost-benefit observations presented herein should be interpreted as indicative rather than universally applicable economic outcomes. Furthermore, with respect to durability classification, the measured RCPT value of 110 Coulombs for M120 concrete indicates exceptionally high resistance to chloride-ion penetration. However, since this value is marginally above the ASTM C1202 threshold of 100 Coulombs commonly associated with the "negligible" permeability category, the result is more accurately described as exhibiting *very low chloride permeability* or *performance approaching the negligible-permeability classification*. This distinction ensures consistency between the reported test data and the adopted classification criteria.

Study Limitations and Scope

Interpret the results presented in this study within the scope of the adopted experimental programme. The reported mechanical and durability properties are intended to provide a comparative evaluation of M40, M80, M100, and M120 concrete under controlled laboratory conditions. To further strengthen experimental rigour, future studies should include comprehensive statistical reporting, including the number of specimens tested for each mix and test condition, individual and averaged measurements, standard deviations, coefficients of variation, and formal statistical comparisons. Such statistical treatment would enable a more rigorous assessment of data variability, repeatability, and confidence in the reported performance trends.

Furthermore, the experimental results reported herein represent laboratory-based observations obtained through the testing programme described in the methodology. They should be distinguished from supporting literature cited for comparison and interpretation. References to previous studies are used solely to contextualise and validate observed trends and are not intended to replace or substitute the experimental findings presented in this work.

The microstructural characterisation component of the investigation was primarily qualitative and based on visual and stereo-microscopic examination of fracture surfaces. These observations provided evidence of reduced visible porosity, improved matrix density, and enhanced interfacial transition zone (ITZ) characteristics in higher-strength mixes. However, advanced characterisation techniques such as Scanning Electron Microscopy (SEM), Energy Dispersive Spectroscopy (EDS), X-Ray Diffraction (XRD), Mercury Intrusion Porosimetry (MIP), and Thermogravimetric Analysis (TGA) would provide more detailed and quantitative information regarding hydration products, pore structure refinement, and microstructural evolution. Therefore, the microstructural findings should be regarded as preliminary qualitative observations rather than a comprehensive microstructural characterisation.

With respect to durability assessment, the M120 concrete exhibited an RCPT value of 110 Coulombs, indicating exceptionally high resistance to chloride ion penetration. However, this value remains marginally above the commonly adopted ASTM C1202 threshold of 100 Coulombs for the negligible-permeability category. Accordingly, the durability performance is more accurately described as **very low chloride permeability** or **approaching the negligible-permeability classification**, rather than strictly negligible permeability.

The economic evaluation presented in this study is intended to illustrate the potential engineering and structural benefits associated with the use of ultra-strength concrete. The comparisons are based primarily on material costs and structural optimisation effects, including reductions in column dimensions, dead load, foundation demand, and potential gains in usable floor area. Consequently, the analysis should not be interpreted as a full life-cycle cost assessment or a complete project-level economic evaluation. A comprehensive economic appraisal would additionally require consideration of reinforcement costs, construction methodology, labour, equipment, maintenance requirements, service-life extension, regional market conditions, and other project-specific factors.

CONCLUSION

- Material Feasibility: Ultra-strength concrete (M80, M100, and M120) can be successfully manufactured using locally available Indian materials, OPC 53 Grade cement, and targeted mineral admixtures under strict quality control, consistent with IS 10262:2019 Section 3 provisions (BIS, 2019).
- Superior Properties: 28-day compressive strengths reached 84 MPa, 104 MPa, and 124 MPa, respectively, with strength gains continuing to 56 days; RCPT results fell to 110 Coulombs for M120, indicating high durability and resistance to chemical ingress.

- Cost-Benefit: While M120 is 244.8% costlier than M40 by material volume, structural column and foundation analysis shows a 71.6% reduction in vertical dead weight and column area, reclaiming substantial commercial carpet area and lowering project lifecycle costs.

Taken together, the experimental results and the surrounding body of literature reviewed in Section 2 indicate that M80–M120 ultra-strength concrete is both technically achievable with Indian materials and economically justified for tall, long-span, and heavily loaded structures once whole-project cost offsets are considered.

REFERENCES

1. ACI Committee 211. (2008). Guide for selecting proportions for high-strength concrete using Portland cement and other cementitious materials (ACI 211.4R-08). American Concrete Institute.
2. ACI Committee 363. (2010). Report on high-strength concrete (ACI 363R-10). American Concrete Institute.
3. ACI Committee 544. (2018). Guide to design with fibre-reinforced concrete (ACI 544.4R-18). American Concrete Institute.
4. Aitkin, P. C. (1998). High-performance concrete. E&FN Spon.
5. Alkaysi, M., El-Tawil, S., Liu, Z., & Hansen, W. (2016). Effects of silica powder and cement type on durability of ultra-high-performance concrete (UHPC). Cement and Concrete Composites, 66, 47–56.
6. ASTM International. (2019). Standard test method for electrical indication of concrete's ability to resist chloride ion penetration (ASTM C1202-19). ASTM International.
7. ASTM International. (2016). Standard specification for steel fibres for fibre-reinforced concrete (ASTM A820/A820M-16). ASTM International.
8. Bache, H. H. (1981). Densified cement/ultra-fine particle-based materials. Aalborg Portland, Denmark.
9. Bentz, D. P., & Aitkin, P. C. (2008). The hidden meaning of water-cement ratio. Concrete International, 30(5), 51–54.
10. British Standards Institution. (2011). Testing concrete – Part 122: Method for determination of water absorption (BS 1881-122:2011). BSI.
11. Bureau of Indian Standards [BIS]. (1999). Concrete admixtures – Specification (IS 9103:1999). Bureau of Indian Standards.
12. Bureau of Indian Standards [BIS]. (2000). Plain and reinforced concrete – Code of practice (IS 456:2000). Bureau of Indian Standards.
13. Bureau of Indian Standards [BIS]. (2003). Silica fume – Specification (IS 15388:2003). Bureau of Indian Standards.
14. Bureau of Indian Standards [BIS]. (2013). Ordinary Portland cement, 53 grade – Specification (IS 12269:2013). Bureau of Indian Standards.
15. Bureau of Indian Standards [BIS]. (2013). Pulverised fuel ash – Specification, Part 1: For use as pozzolana in cement, cement mortar and concrete (IS 3812 (Part 1):2013). Bureau of Indian Standards.
16. Bureau of Indian Standards [BIS]. (2016). Coarse and fine aggregate for concrete – Specification (Third Revision) (IS 383:2016). Bureau of Indian Standards.
17. Bureau of Indian Standards [BIS]. (2018). Ground granulated blast furnace slag – Specification (IS 16714:2018). Bureau of Indian Standards.
18. Bureau of Indian Standards [BIS]. (2019). Concrete mix proportioning – Guidelines (Second Revision) (IS 10262:2019). Bureau of Indian Standards.
19. Bureau of Indian Standards [BIS]. (1959, reaffirmed with amendments). Method of tests for strength of concrete (IS 516:1959). Bureau of Indian Standards.
20. Bureau of Indian Standards [BIS]. (2020). Method of test for determination of rapid chloride permeability of concrete (IS 17452:2020). Bureau of Indian Standards.
21. Deutsches Institut für Normung. (1991). Testing concrete – Determination of the depth of penetration of water under pressure, Part 5 (DIN 1048-5:1991). DIN.
22. Domene, P. L. (2007). A review of the hardened mechanical properties of self-compacting concrete. Cement and Concrete Composites, 29(1), 1–12.
23. Federal Highway Administration [FHWA]. (2013). Design and construction guidelines for ultra-high-performance concrete (Report No. FHWA-HRT-13-060). U.S. Department of Transportation.

24. Graybeal, B. (2006). Material property characterisation of ultra-high performance concrete (Report No. FHWA-HRT-06-103). Federal Highway Administration.
25. Habel, K., Viviani, M., Demarie, E., & Brawlier, E. (2006). Development of the mechanical properties of an ultra-high-performance fibre reinforced concrete (UHPFRC). Cement and Concrete Research, 36(7), 1362–1370.
26. Kumar, R., & Bhattacharjee, B. (2003). Porosity, pore size distribution and in situ strength of concrete. Cement and Concrete Research, 33(1), 155–164.
27. Mehta, P. K., & Monteiro, P. J. M. (2014). Concrete: Microstructure, properties, and materials (4th ed.). McGraw-Hill Education.
28. Neville, A. M. (2011). Properties of concrete (5th ed.). Pearson Education.
29. Richard, P., & Cheyrezy, M. (1995). Composition of reactive powder concretes. Cement and Concrete Research, 25(7), 1501–1511.
30. Rossi, P., Arca, A., Parant, E., & Fakhri, P. (2005). Bending and compressive behaviours of a new cement composite. Cement and Concrete Research, 35(1), 27–33.
31. Santra, A., & Mukherjee, B. (2023). Review paper on experimental study of ultra-high strength concrete (UHSC). International Journal of Engineering Inventions, 12(7), 123–134.
32. Shi, C., Wu, Z., Xiao, J., Wang, D., Huang, Z., & Fang, Z. (2015). A review on ultra-high performance concrete: Part I. Raw materials and mixture design. Construction and Building Materials, 96, 368–377.
33. Sobolev, K. (2004). The development of a new method for the proportioning of high-performance concrete mixtures. Cement and Concrete Composites, 26(7), 901–907.
34. Sreenivasulu, A., & Srinivasa Rao, K. (2012). Design of M100 grade concrete (ACI method). Global Journal of Engineering & Applied Sciences, 2(2), 183–185.
35. Whiting, D. (1981). Rapid determination of the chloride permeability of concrete (Report No. FHWA/RD-81/119). Federal Highway Administration.
36. Wille, K., Naaman, A. E., & Parra-Montesinos, G. J. (2011). Ultra-high-performance concrete with compressive strength exceeding 150 MPa: A simpler way. ACI Materials Journal, 108(1), 46–54.
37. Yu, R., Spiesz, P., & Brouwers, H. J. H. (2014). Mix design and properties assessment of Ultra-High-Performance Fibre Reinforced Concrete (UHPFRC). Cement and Concrete Research, 56, 29–39.